Robust Co-Planning of Energy Storage and Transmission Line with Mixed Integer Recourse

Siyuan Wang, Guangchao Geng, *Member, IEEE*, Quanyuan Jiang, *Member, IEEE*

***Abstract*—Energy storage is a potential planning option to relieve transmission congestion caused by increasing penetration of renewable energy. This paper presents a robust formulation for energy storage and transmission line co-planning, considering binary variables that represent energy storage statuses in the recourse problem. In order to solve this model, an improved nested column and constraint generation (nested C&CG) algorithm is used to cope with numerical issues caused by new binary variables, big-M constraints, and the enormous size of the problem. Case studies of a modified Garver's 6-bus system and a practical Chinese 196-bus system were used to assess the effectiveness of the proposed approach. The numerical results indicate that energy storage is more economical for relieving the transmission line congestion when the transmission distance is relatively long.**

***Index Terms*—energy storage, transmission line, co-planning, renewable power, uncertainty, mixed integer recourse**

NOMENCLATURE

Indices and Sets:

b, i	Index of buses and devices in the power system
j	Index of energy storage types
k	Index of regions
s	Index of scenarios
t	Index of time periods
$\Omega_{\mathrm{w}}, \Omega_{\mathrm{g}}$	Set of wind/solar farms and generators
Ω_{d}	Set of loads
$\Omega_{\mathrm{es(nes)}}^{\mathrm{typ}}$	Set of existing (candidate) energy storage types
$\Omega^{\mathrm{bus}}(j)$	Set of buses or candidate buses for energy storage type j
$\Omega_{\mathrm{l(nl)}}$	Set of existing (candidate) AC transmission lines
$\Omega_{\mathrm{ldc(nldc)}}$	Set of existing (candidate) DC transmission lines
$\Omega_*^b, \Omega_*^{RG_k}$	Set of equipment * at bus b or in region k

Parameters:

N_s	Number of scenarios
N_t	Number of time periods in each daily scenario
$\tau(s)$	Number of days in a year represented by the base case scenario s
C_i^{cons}	Annualized construction cost of transmission line i
$C_{\mathrm{line}\,i}$	Annualized construction cost per unit length of transmission line i
$C_{\mathrm{conv}\,i}$	Annualized converter construction cost of HVDC i
l_i	Length of transmission line i
$\alpha_{j,b}, \beta_{j,b}$	Construction cost per unit power capacity and per unit energy capacity of storage type j at bus b
$\chi_{j,b}$	Fixed construction cost of storage type j at bus b
$C_{i,s,t}^{\mathrm{load}}$	Load shedding cost of load i at time t in scenario s
$C_{i,s,t}^{\mathrm{gen}}$	Operation cost of generator i at time t in scenario s
$C_{j,b,s,t}^{\mathrm{dc(ch)}}$	Charge (discharge) operation cost of energy storage type j at bus b and time t in scenario s
$w_{i,s,t}$	Power output of renewable generation i at time t in scenario s
$d_{i,s,t}$	Power output of load i at time t in scenario s
$d_{i,s,t}^{\mathrm{c\,max}}$	Maximum load shedding power of load i at time t in scenario s
φ_k	Maximum ratio of load shedding in region k
x_i	Reactance of transmission line i
F_i	Capacity of transmission line i
M_i	Big M value of transmission line i
$\overline{P}_i, \underline{P}_i$	Maximum and minimum output of generator i
RU_i, RD_i	Ramp up and down capability of generator i
$P_{j,b}^{\max}, E_{j,b}^{\max}$	Maximum power and energy capacity of candidate energy storage type j at bus b
ϕ_j	Bound factor for power capacity of storage type j
δ_j	Self-discharge rate of energy storage type j
$\eta_j^{\mathrm{ch(dc)}}$	Charge (discharge) efficiency of storage type j
$e_{j,b,s,0}$	Initial energy stored of energy storage type j at bus b and scenario s
$\overline{\gamma}(\underline{\gamma})_{j,b,s,t}$	Upper (lower) bound factor for energy stored of storage type j at bus b and time t in scenario s
$\gamma_{j,b,s,0}$	Initial factor of energy stored of energy storage type j at bus b in scenario s

Decision Variables:

$z_{j,b}, z_i$	Binary variable of investment decision for energy storage type j at bus b and transmission line i
$P_{j,b}, E_{j,b}$	Power and energy capacity of energy storage type j at bus b, which is a parameter for existing storage
$d_{i,s,t}^{\mathrm{c}}$	Load shedding of load i at time t in scenario s
$p_{i,s,t}$	Output power of generator i at time t in scenario s
$p_{j,b,s,t}$	Output power of energy storage type j at bus b and time t in scenario s
$f_{i,s,t}$	Flow of transmission line i at time t in scenario s
$\theta_{b,s,t}$	Voltage angle of bus b at time t in scenario s
$u_{j,b,s,t}^{\mathrm{ch(dc)}}$	Binary charge (discharge) status of energy storage type j at bus b and time t in scenario s
$p_{j,b,s,t}^{\mathrm{ch(dc)}}$	Charge (discharge) power of energy storage type j at bus b and time t in scenario s
$e_{j,b,s,t}$	Energy stored of energy storage type j at bus b and time t in scenario s

S. Wang, G. Geng and Q. Jiang are with College of Electrical Engineering, Zhejiang University, Hangzhou 310027, China. (email: sywang@zju.edu.cn; ggc@zju.edu.cn; jqy@zju.edu.cn).

This article has been accepted for publication in IEEE Transactions on Power Systems. DOI: 10.1109/TPWRS.2019.2914276.

Compact Representation:

M_σ	Penalty coefficient for the slack variable σ
$a_{1(2,3)}$	Vector of coefficients in the objective function
$A_{1(2,3)}^{\text{ie(eq)}}$	Matrix of coefficients in inequality (equality) constraints
$A_{u(\sigma)}$	Matrix of coefficients for variable u (σ)
$b^{\text{ie(eq)}}$	Vector of constant terms in inequality (equality) constraints
U	Uncertainty set
σ	Slack variable for transmission line capacity
$x, y_{\text{d}}, y_{\text{c}}$	Vectors of planning decision variables, discrete and continuous operational variables
u	Vector of the uncertain renewable power
$.^{\text{bc}}$	Vector associated with base case scenarios
$\hat{.}$	Fixed value of decision variables
κ, π, η	Ancillary variables defined in the algorithm
λ, μ	Dual variables for inequalities and equalities
$\varsigma(\cdot)$	Function defined in the algorithm

I. Introduction

THE variability and uncertainty of renewable energy sources threaten the security of supply in modern power systems. The increasing penetration of renewable generation might increase transmission line congestion, which presents a significant challenge for system planners. Besides planning new transmission lines, energy storage is also an option for relieving transmission congestion by decreasing the variability of renewable generation. Both transmission expansion planning [1-6] and energy storage planning [7-9] have been extensively investigated in the literature for decades. Recently, co-planning of energy storage and transmission line has gained increasing attention in [10-13], which indicates co-planning is useful for reducing the overall required investment.

In the scope of uncertainty quantification and modeling, stochastic programming and robust optimization are two mainstream methodologies used for solving planning problems. Stochastic co-planning of energy storage and transmission line under wind power uncertainty was proposed in [14, 15], wherein co-planning was found to improve the system's ability to alleviate transmission congestion and integrate wind power. A robust optimization-based method for joint transmission and energy storage expansion planning with transmission switching was presented in [16], which guarantees the existence of an operation scheme in any instance given a predefined uncertainty set. The pros and cons of both stochastic and robust approaches were compared in several applications [17, 18]. In addition, stochastic programming has the advantage of taking the expectations of some concerned measures into consideration. The quality of investment decision can be further improved by increasing the number of sampling scenarios, which would result in the actual costs incurred by the system decreasing. In this planning application, we choose the robust optimization approach due to the unavailability of accurate statistical models, which usually occurs in practical applications [19].

In the literature, most energy storage formulations contain binary variables that indicate charge and discharge statuses, which are difficult to eliminate in general. They are defined to model different costs and efficiencies in charging and discharging processes, as well as to model the disjunctive relationship between charge and discharge statuses. It should be noted that these binary variables are operational variables, so they should be determined in the system operational phase after making a planning decision. In previous work on two-stage robust planning with energy storage [16, 19], these binary variables were taken as first stage variables (first and second stage variables are 'here and now' and 'wait and see' variables, respectively). Although these formulations can reduce computational burden, determining energy storage statuses in the planning stage rather than the operational stage, may limit its flexibility to address renewable power uncertainty, which might lead to redundant investment results or even make the problem infeasible (as shown in the case study in Section IV). In this work, a robust formulation for energy storage and transmission line co-planning with binary variables that indicate energy storage statuses in the recourse problem (i.e., in the operational stage) is proposed.

From an algorithmic perspective, solving a robust mixed integer linear programming (MILP) problem with mixed integer recourse is challenging. Currently, most two-stage robust optimization problems in power system applications contain linear programming (LP) or convex recourse problems, such as robust transmission expansion planning in [20], robust generation expansion planning in [21], and robust unit commitment in [22]. These models can be efficiently solved using algorithms based on strong duality theory, but such algorithms cannot be extended to problems with mixed integer recourse. Reference [23] extended the work of [24], and presented a nested column and constraint generation (nested C&CG) algorithm, which is an exact algorithm for solving two-stage robust optimization with mixed integer recourse problems. In light of this work, we exploit the framework of nested C&CG algorithm to solve the robust co-planning problem with mixed integer recourse.

In our numerical practice, the slave sub-problem in the basic version nested C&CG algorithm in [23] (denoted as the 'basic version' hereafter) suffers from severe computational issues. Given a large number of inequality constraints, linearization of the complementary slackness condition in the basic version algorithm introduced numerous new binary variables and big-M constraints, making the problem unscalable. Therefore, an improved strategy is used to address the computational efficiency and make the problem solvable for real-world co-planning problems.

The contributions of this work include:

1) A robust formulation for energy storage and transmission line co-planning is proposed with binary variables that indicate energy storage statuses in the recourse problem. This formulation offers reasonable investment decisions for energy storage (i.e., power/energy capacity, location, and technology type) and transmission line under renewable power uncertainty.
2) An improved nested C&CG algorithm is used to solve the two-stage robust optimization problem with mixed integer recourse. The computational issues caused by new binary variables, big-M constraints, and enormous size in the basic version algorithm are addressed for this certain problem.
3) Effect of energy storage on relieving transmission line congestion is analyzed in the case study. A two-region practical power system is presented to analyze the economic plausibility of energy storage investment for reducing investment in transmission lines.

II. Problem Formulation

The co-planning problem aims to offer reasonable investment decisions for energy storages and transmission lines in a unified formulation. In this section, a deterministic formulation is presented first, which is then extended to a robust formulation.

A. Deterministic Formulation

1) Objective Function

The objective function is expressed in (1), which considers annualized investment cost (*term a* for transmission lines, *term b* for energy storages) and operational cost (*term c* for generators, *term e* for energy storages and *term d* for load shedding penalties). The investment cost of candidate energy storage is the sum of power capacity cost, energy capacity cost, and fixed cost.

$$\begin{aligned}\min\ & \underbrace{\sum_{i\in\Omega_{\mathrm{nl}}\cup\Omega_{\mathrm{nldc}}} C_i^{\mathrm{cons}} z_i}_{term\ a} + \underbrace{\sum_{j\in\Omega_{\mathrm{nes}}^{\mathrm{typ}},b\in\Omega^{\mathrm{bus}}(j)} \left(\alpha_{j,b}P_{j,b}+\beta_{j,b}E_{j,b}+\chi_{j,b}z_{j,b}\right)}_{term\ b} \\ & + \underbrace{\sum_{i\in\Omega_{\mathrm{g}}}\sum_{s\in S}\sum_{t=1}^{N_t}\tau(s)\cdot\left(C_{i,s,t}^{\mathrm{gen}}p_{i,s,t}\right)}_{term\ c} + \underbrace{\sum_{i\in\Omega_{\mathrm{d}}}\sum_{s\in S}\sum_{t=1}^{N_t}\tau(s)\cdot\left(C_{i,s,t}^{\mathrm{load}}d_{i,s,t}^{\mathrm{c}}\right)}_{term\ d} \\ & + \underbrace{\sum_{j\in\Omega_{\mathrm{es}}^{\mathrm{typ}}\cup\Omega_{\mathrm{nes}}^{\mathrm{typ}},b\in\Omega^{\mathrm{bus}}(j)}\sum_{s\in S}\sum_{t=1}^{N_t}\tau(s)\cdot\left(C_{j,b,s,t}^{\mathrm{dc}}p_{j,b,s,t}^{\mathrm{dc}}+C_{j,b,s,t}^{\mathrm{ch}}p_{j,b,s,t}^{\mathrm{ch}}\right)}_{term\ e}\end{aligned} \tag{1}$$

2) System Constraints

The system constraints ensure power flow balance at each bus based on Kirchhoff's current law, which are expressed in (2).

$$\begin{aligned}&\sum_{i\in\Omega_{\mathrm{l}}^{bt}\cup\Omega_{\mathrm{nl}}^{bt}\cup\Omega_{\mathrm{ldc}}^{bt}\cup\Omega_{\mathrm{nldc}}^{bt}} f_{i,s,t} - \sum_{i\in\Omega_{\mathrm{l}}^{bf}\cup\Omega_{\mathrm{nl}}^{bf}\cup\Omega_{\mathrm{ldc}}^{bf}\cup\Omega_{\mathrm{nldc}}^{bf}} f_{i,s,t} + \sum_{i\in\Omega_{\mathrm{g}}^{b}} p_{i,s,t} \\ &+ \sum_{j\in\Omega_{\mathrm{es}}^{\mathrm{typ}}\cup\Omega_{\mathrm{nes}}^{\mathrm{typ}}} p_{j,b,s,t} = \sum_{i\in\Omega_{\mathrm{d}}^{b}}\left(d_{i,s,t}^{\mathrm{c}}-d_{i,s,t}^{\mathrm{c}}\right) - \sum_{i\in\Omega_{\mathrm{w}}^{b}} w_{i,s,t} \quad \forall b,s,t\end{aligned} \tag{2}$$

3) Wind/Solar Curtailment and Load Shedding Constraints

According to Article 14 of the Renewable Energy Law of P. R. China [25], the full amount purchasing of renewable energy power is guaranteed, and energy storage technologies shall be developed and used to improve the integration of renewable energy. Thus, wind/solar curtailment constraints are not modeled. Load shedding constraints are modeled according to the Regulations on Emergency Handling, Investigation and Disposal of Electric Power Safety Accidents promulgated by State Council of P. R. China [26, 27], which restricts load shedding proportions for different types of regions. Equation (3) provides the load shedding bounds for each load, and (4) limits the load shedding proportion for region *k*.

$$0 \le d_{i,s,t}^{\mathrm{c}} \le d_{i,s,t}^{\mathrm{c\,max}} \quad \forall i\in\Omega_{\mathrm{d}},s,t \tag{3}$$

$$\sum_{i\in\Omega_{\mathrm{d}}^{RGk}} d_{i,s,t}^{\mathrm{c}} \le \varphi_k \sum_{i\in\Omega_{\mathrm{d}}^{RGk}} d_{i,s,t} \quad \forall k,s,t \tag{4}$$

Wind/solar curtailment and load shedding constraints can be easily modeled or modified according to the regulations in different power grids.

4) Transmission Line Constraints

The disjunctive model based on DC power flow is adopted for existing and candidate transmission lines, where the big-M value is determined using the method in [4]. Equations (5) and (7) are branch flow equations that are applicable for existing and candidate AC transmission lines, respectively. Equations (6) and (8) bound the branch flows by the capacities of existing and candidate transmission lines, respectively, which are applicable for both AC and DC transmission lines.

$$f_{i,s,t} = \left(\theta_{bf(i),s,t}-\theta_{bt(i),s,t}\right)\Big/x_i \quad \forall i\in\Omega_{\mathrm{l}},s,t \tag{5}$$

$$-F_i \le f_{i,s,t} \le F_i \quad \forall i\in\Omega_{\mathrm{l}}\cup\Omega_{\mathrm{ldc}},s,t \tag{6}$$

$$\left| f_{i,s,t} - \left(\theta_{bf(i),s,t}-\theta_{bt(i),s,t}\right)\Big/x_i \right| \le M_i\left(1-z_i\right) \quad \forall i\in\Omega_{\mathrm{nl}},s,t \tag{7}$$

$$-z_iF_i \le f_{i,s,t} \le z_iF_i \quad \forall i\in\Omega_{\mathrm{nl}}\cup\Omega_{\mathrm{nldc}},s,t \tag{8}$$

5) Generator Constraints

Maximum and minimum outputs from an individual generator are described by (9). Equation (10) provides constraints for upward and downward ramp rates of generators.

$$\underline{P}_i \le p_{i,s,t} \le \bar{P}_i \quad \forall i\in\Omega_{\mathrm{g}},s,t \tag{9}$$

$$-RD_i \le p_{i,s,t+1}-p_{i,s,t} \le RU_i \quad \forall i\in\Omega_{\mathrm{g}},s,t\in\left[1,N_t-1\right] \tag{10}$$

6) Energy Storage Constraints

Both existing and candidate energy storages are modeled in this subsection. Equations (11) and (12) ensure charge power $p_{j,b,s,t}^{\mathrm{dc}}$ and discharge power $p_{j,b,s,t}^{\mathrm{ch}}$ from existing energy storage within their corresponding bounds. In particular, $p_{j,b,s,t}^{\mathrm{dc}}$ ($p_{j,b,s,t}^{\mathrm{ch}}$) is set to zero if the corresponding status variable $u_{j,b,s,t}^{\mathrm{dc}}$ ($u_{j,b,s,t}^{\mathrm{ch}}$) is zero. However, for candidate energy storages, the product terms of power capacities $P_{j,b}$ and status variables will introduce nonlinearity into the formulation. Note that the power capacity $P_{j,b}$ is a decision variable for candidate storage, while a parameter for existing storage. Thus, $P_{j,b}^{\max}$, which is an upper bound on candidate energy storage power capacity, is used to replace $P_{j,b}$ in (13) and (14). Additional inequalities guarantee $p_{j,b,s,t}^{\mathrm{dc}}$ and $p_{j,b,s,t}^{\mathrm{ch}}$ are not greater than $P_{j,b}$. Equation (15) defines the network injection power $p_{j,b,s,t}$ of each energy storage. Equation (16) establishes a disjunctive inequality for statuses $u_{j,b,s,t}^{\mathrm{dc}}$ and $u_{j,b,s,t}^{\mathrm{ch}}$. Equation (17) models the relation between energy status $e_{j,b,s,t}$ and charge/discharge power. Equations (18)-(20) bound $e_{j,b,s,t}$ at the initial, intermediate and final time periods, respectively. Similar to $P_{j,b}$, the energy capacity $E_{j,b}$ is a parameter for existing storage, while a variable for candidate storage. Equations (21) and (22) provide upper bounds for power and energy capacities of candidate energy storages if applicable. In addition, candidate buses rely on the types of energy storages, i.e., $b\in\Omega^{\mathrm{bus}}(j)$.

$$0 \le p_{j,b,s,t}^{\mathrm{dc}} \le \phi_j P_{j,b} u_{j,b,s,t}^{\mathrm{dc}} \quad \forall j\in\Omega_{\mathrm{es}}^{\mathrm{typ}},b,s,t \tag{11}$$

$$0 \le p_{j,b,s,t}^{\mathrm{ch}} \le \phi_j P_{j,b} u_{j,b,s,t}^{\mathrm{ch}} \quad \forall j\in\Omega_{\mathrm{es}}^{\mathrm{typ}},b,s,t \tag{12}$$

$$0 \le p_{j,b,s,t}^{\mathrm{dc}} \le \phi_j P_{j,b}^{\max} u_{j,b,s,t}^{\mathrm{dc}},\ p_{j,b,s,t}^{\mathrm{dc}} \le \phi_j P_{j,b} \ \forall j\in\Omega_{\mathrm{nes}}^{\mathrm{typ}},b,s,t \tag{13}$$

$$0 \le p_{j,b,s,t}^{\mathrm{ch}} \le \phi_j P_{j,b}^{\max} u_{j,b,s,t}^{\mathrm{ch}},\ p_{j,b,s,t}^{\mathrm{ch}} \le \phi_j P_{j,b} \ \forall j\in\Omega_{\mathrm{nes}}^{\mathrm{typ}},b,s,t \tag{14}$$

$$p_{j,b,s,t} = p_{j,b,s,t}^{\mathrm{dc}} - p_{j,b,s,t}^{\mathrm{ch}}, \quad \forall j\in\Omega_{\mathrm{es}}^{\mathrm{typ}}\cup\Omega_{\mathrm{nes}}^{\mathrm{typ}},b,s,t \tag{15}$$

$$u_{j,b,s,t}^{\mathrm{ch}} + u_{j,b,s,t}^{\mathrm{dc}} \le z_{j,b}, \quad \forall j\in\Omega_{\mathrm{es}}^{\mathrm{typ}}\cup\Omega_{\mathrm{nes}}^{\mathrm{typ}},b,s,t \tag{16}$$

$$\begin{aligned}e_{j,b,s,t} = \left(1-\delta_j\right)e_{j,b,s,t-1} + \eta_j^{\mathrm{ch}}\cdot p_{j,b,s,t}^{\mathrm{ch}} - 1\Big/\eta_j^{\mathrm{dc}}\cdot p_{j,b,s,t}^{\mathrm{dc}} \\ \forall j\in\Omega_{\mathrm{es}}^{\mathrm{typ}}\cup\Omega_{\mathrm{nes}}^{\mathrm{typ}},b,s,t\end{aligned} \tag{17}$$

$$e_{j,b,s,0} = \gamma_{j,b,s,0}E_{j,b}, \quad \forall j\in\Omega_{\mathrm{es}}^{\mathrm{typ}}\cup\Omega_{\mathrm{nes}}^{\mathrm{typ}},b,s \tag{18}$$

$$\underline{\gamma}_{j,b,s,t}E_{j,b} \le e_{j,b,s,t} \le \bar{\gamma}_{j,b,s,t}E_{j,b}, \ \forall j\in\Omega_{\mathrm{es}}^{\mathrm{typ}}\cup\Omega_{\mathrm{nes}}^{\mathrm{typ}},b,s,t \tag{19}$$

$$\underline{\gamma}_{j,b,s,N_t}E_{j,b} \le e_{j,b,s,N_t} \le \bar{\gamma}_{j,b,s,N_t}E_{j,b}, \ \forall j\in\Omega_{\mathrm{es}}^{\mathrm{typ}}\cup\Omega_{\mathrm{nes}}^{\mathrm{typ}},b,s \tag{20}$$

$$P_{j,b} \le P_{j,b}^{\max} z_{j,b} \quad \forall j\in\Omega_{\mathrm{nes}}^{\mathrm{typ}},b \tag{21}$$

$$E_{j,b} \le E_{j,b}^{\max} z_{j,b} \quad \forall j \in \Omega_{\text{nes}}^{\text{typ}}, b \tag{22}$$

B. Robust Formulation

The deterministic co-planning problem is modeled as an MILP formulation with objective function (1) and constraints (2)-(22). For the sake of convenient demonstration in the remainder part of this paper, its compact formulation is expressed as shown in (23).

$$\begin{aligned} \min_{x,y_{\text{d}},y_{\text{c}}} \quad & \underbrace{a_1^T x}_{\text{term } a,b \text{ in Eqn. (1)}} + a_2^T y_{\text{d}} + \underbrace{a_3^T y_{\text{c}}}_{\text{term } c,d,e \text{ in Eqn. (1)}} \\ s.t. \quad & A_1^{\text{ie}} x + A_2^{\text{ie}} y_{\text{d}} + A_3^{\text{ie}} y_{\text{c}} \le b^{\text{ie}} \\ & A_1^{\text{eq}} x + A_2^{\text{eq}} y_{\text{d}} + A_3^{\text{eq}} y_{\text{c}} = b^{\text{eq}} + A_u \hat{u} \end{aligned} \tag{23}$$

In (23), x defines the vector of planning decision variables (i.e., z_l for transmission lines, and P_i, E_i, z_i for energy storages). y_{d} is the vector of discrete operational variables (i.e., $u_{i,s,t}^{\text{ch}}$ and $u_{i,s,t}^{\text{dc}}$ of energy storages). y_{c} denotes the vector of continuous operational variables (i.e., operational variables excluding $u_{i,s,t}^{\text{ch}}$ and $u_{i,s,t}^{\text{dc}}$). u is the vector of uncertain renewable generation $w_{i,s,t}$, which is fixed in the deterministic formulation. The correspondence of terms between the detailed and the compact form of the objective function is also marked in (1) and (23). Note that $a_2 = \mathbf{0}$ in this planning application. The inequality constraint in (23) corresponds to (3)-(4), (6)-(14), (16) and (19)-(22), while the equality constraint represents (2), (5), (15), and (17)-(18).

The two-stage robust formulation expressed in (24) is established considering the uncertainty of renewable generation u, where x contains the first stage variables determined in the planning phase, while y_{c} and y_{d} are the second stage variables that are adjustable after the realization of first stage variables. As a long-term planning problem, system operational cost is estimated from the base case scenarios. Meanwhile, the feasibility of the worst-case scenario is ensured under the load shedding limits of grid codes. The variables associated with the base case scenarios are marked with superscript *bc*.

$$\begin{aligned} \min_{x,y_{\text{d}}^{\text{bc}},y_{\text{c}}^{\text{bc}}} \quad & \left[a_1^T x + a_2^T y_{\text{d}}^{\text{bc}} + a_3^T y_{\text{c}}^{\text{bc}} + \max_{u \in U} \min_{y_{\text{d}},y_{\text{c}},\sigma \ge 0} \left(M_\sigma \cdot \sigma \right) \right] \\ s.t. \quad & A_1^{\text{ie}} x + A_2^{\text{ie}} y_{\text{d}}^{\text{bc}} + A_3^{\text{ie}} y_{\text{c}}^{\text{bc}} \le b^{\text{ie}} \\ & A_1^{\text{eq}} x + A_2^{\text{eq}} y_{\text{d}}^{\text{bc}} + A_3^{\text{eq}} y_{\text{c}}^{\text{bc}} = b^{\text{eq}} + A_u \hat{u}^{\text{bc}} \\ & A_1^{\text{ie}} x + A_2^{\text{ie}} y_{\text{d}} + A_3^{\text{ie}} y_{\text{c}} \le b^{\text{ie}} + A_\sigma \sigma \\ & A_1^{\text{eq}} x + A_2^{\text{eq}} y_{\text{d}} + A_3^{\text{eq}} y_{\text{c}} = b^{\text{eq}} + A_u u \end{aligned} \tag{24}$$

In (24), the slack variable σ is introduced to prevent infeasibility in the solution process, and the penalty term $M_\sigma \cdot \sigma$ is added to the objective function. In detail, (6) and (8) are slacked, and the expressions are shown in (25)-(27).

$$-F_l - \sigma \le f_{l,s,t} \le F_l + \sigma \quad \forall l \in \Omega_{\text{l}} \bigcup \Omega_{\text{ldc}}, s, t \tag{25}$$

$$-z_l F_l - \sigma \le f_{l,s,t} \le z_l F_l + \sigma \quad \forall l \in \Omega_{\text{nl}} \bigcup \Omega_{\text{nldc}}, s, t \tag{26}$$

$$\sigma \ge 0 \tag{27}$$

In contrast to most previous robust formulations for determining energy storage statuses in the planning phase, which might lead to redundant investment or even infeasibility, (24) is a two-stage robust optimization formulation with mixed integer recourse.

III. Improved Nested C&CG Algorithm

In this section, an improved nested C&CG algorithm is used to solve the proposed formulation. In [23], the original problem is converted to a four-level min-max-min-min problem, in which the third stage minimization contains binaries and the last stage is an LP problem. The LP minimization problem is equivalent to a set of linear equations with complementary slackness constraints by applying Karush-Kuhn-Tucker (KKT) conditions, which is then further transformed to mixed integer linear equations using the big-M method. Finally, the resultant min-max-min problem is solved nestedly with the C&CG algorithm. This exploits the advantage of the C&CG algorithm, which is indifferent to the types of variables in the recourse problem, while Benders-dual algorithms require that the recourse be convex [24].

This solution strategy in the basic version is an exact algorithm for two-stage robust optimization. However, it suffers from numerical issues when the number of inequality constraints is large. In practical applications, big-M linearization of complementary slackness conditions would introduce a large number of new binary variables and big-M constraints, making the problem unscalable. The improved algorithm adopts the framework of the basic version algorithm, which operates under two master-slave frameworks, i.e., the outer loop and inner loop. The improvement is made in the inner loop to address computational issues.

A. Outer Loop

The outer loop decomposes the original problem (24) into master and slave sub-problems using the C&CG algorithm, which offers updated bounds for the original problem in each iteration. Equation (28) is the master problem (MP) of the outer loop, which is used to compute lower bounds for the objective function in (24). Equation (29) is the slave problem (SP) of the outer loop, which provides the upper bounds.

$$\begin{aligned} \text{(MP)} \quad & \min_{x,y_{\text{d}}^{\text{bc}},y_{\text{c}}^{\text{bc}},y_{\text{d}}^{(i)},y_{\text{c}}^{(i)}} a_1^T x + a_2^T y_{\text{d}}^{\text{bc}} + a_3^T y_{\text{c}}^{\text{bc}} \\ & s.t. \quad A_1^{\text{ie}} x + A_2^{\text{ie}} y_{\text{d}}^{\text{bc}} + A_3^{\text{ie}} y_{\text{c}}^{\text{bc}} \le b^{\text{ie}} \\ & \quad A_1^{\text{eq}} x + A_2^{\text{eq}} y_{\text{d}}^{\text{bc}} + A_3^{\text{eq}} y_{\text{c}}^{\text{bc}} = b^{\text{eq}} + A_u \hat{u}^{\text{bc}} \\ & \quad A_1^{\text{ie}} x + A_2^{\text{ie}} y_{\text{d}}^{(i)} + A_3^{\text{ie}} y_{\text{c}}^{(i)} \le b^{\text{ie}} \\ & \quad A_1^{\text{eq}} x + A_2^{\text{eq}} y_{\text{d}}^{(i)} + A_3^{\text{eq}} y_{\text{c}}^{(i)} = b^{\text{eq}} + A_u \hat{u}^{(i)} \\ & \quad i = 1, 2, ..., I \end{aligned} \tag{28}$$

$$\begin{aligned} \text{(SP)} \quad & \hat{\kappa}^{(I)} + \max_{u \in U} \min_{y_{\text{d}},y_{\text{c}},\sigma \ge 0} \left(M_\sigma \cdot \sigma \right) \\ & s.t. \quad A_2^{\text{ie}} y_{\text{d}} + A_3^{\text{ie}} y_{\text{c}} - A_\sigma \sigma \le b^{\text{ie}} - A_1^{\text{ie}} \hat{x}^{(I)} \\ & \quad A_2^{\text{eq}} y_{\text{d}} + A_3^{\text{eq}} y_{\text{c}} = b^{\text{eq}} - A_1^{\text{eq}} \hat{x}^{(I)} + A_u u \end{aligned} \tag{29}$$

where,

$$\hat{\kappa}^{(I)} = a_1^T \hat{x}^{(I)} + a_2^T \hat{y}_{\text{d}}^{\text{bc}(I)} + a_3^T \hat{y}_{\text{c}}^{\text{bc}(I)} \tag{30}$$

B. Inner Loop

In fact, the SP in (29) is a tri-level max-min-min problem. Reference [23] decomposed it into an MILP upper level problem and an MILP lower level problem in the inner loop. The MILP upper level problem is formulated by transforming complementary slackness constraints in the KKT conditions into a linearized formulation using the big-M method. Although this conversion works well in the small-scale rostering problem under uncertain demands as shown in [23], numerical difficulties faced in practical planning problems are mainly in three-folds:

1) Linearization of complementary slackness constraints introduces a number of new binary variables, whose

dimension equals the number of inequalities in the deterministic formulation. However, our co-planning problem contains a large number of inequalities. Thus, the MILP may become intractable for the large-scale problem.

2) A large number of big-M constraints are also introduced. The number of big-M constraints is twice the number of inequalities in the deterministic formulation. What is worse, it is difficult to determine proper big-M values, especially for constraints with dual variables. Conservative bounds might cause the MILP solver to exhibit poor numerical performance, while too small bounds might cause the big-M conversion to be inequivalent.

3) As the new binary variables and big-M constraints increase during the inner loop, the issues in 1) and 2) might become even worse.

In this paper, the SP in (29) is again decomposed into upper and lower level problems using the C&CG approach. The upper level of the slave problem (SP-U) is shown in (31), which is used to compute the upper bounds. The lower level of the slave problem (SP-L) is shown in (33), which offers lower bounds for the objective function of the SP.

The improved strategy is used to prevent the KKT conditions from being exploited. Aside from the KKT conditions, another option to cope with the inner minimization problem is duality. In contrast to the SP-U in the basic version algorithm, the inner minimization problem is converted to its dual problem, as shown in (31) and (32). This conversion does not require use of the KKT conditions, thus a large number of big-M constraints is not required and the overall problem size is reduced.

$$\text{(SP-U)}\quad \pi^{(J)} = \hat{\kappa}^{(I)} + \max_{\eta,u}\ \eta$$
$$s.t.\quad \eta \le \varsigma\left(\hat{x}^{(I)}, \hat{y}_{\mathrm{d}}^{(j)}, u\right) \tag{31}$$
$$u \in U$$
$$\forall j = 1,2,...,J$$

where,

$$\varsigma\left(\hat{x}^{(I)}, \hat{y}_{\mathrm{d}}^{(j)}, u\right) = \max_{\lambda^{(j)},\mu^{(j)}} \left[\left(b^{\mathrm{ie}} - A_1^{\mathrm{ie}}\hat{x}^{(I)} - A_2^{\mathrm{ie}}\hat{y}_{\mathrm{d}}^{(j)}\right)^T \lambda^{(j)} + \left(b^{\mathrm{eq}} - A_1^{\mathrm{eq}}\hat{x}^{(I)} - A_2^{\mathrm{eq}}\hat{y}_{\mathrm{d}}^{(j)} + A_u u\right)^T \mu^{(j)}\right]$$
$$s.t.\quad \lambda^{(j)T}A_3^{\mathrm{ie}} + \mu^{(j)T}A_3^{\mathrm{eq}} = 0$$
$$-\lambda^{(j)T}A_\sigma \le M_\sigma$$
$$\lambda^{(j)} \le 0 \tag{32}$$

$$\text{(SP-L)}\quad \hat{\kappa}^{(I)} + \min_{y_{\mathrm{d}}^{(J)}, y_{\mathrm{c}}^{(J)}, \sigma^{(J)} \ge 0} \left(M_\sigma \cdot \sigma^{(J)}\right)$$
$$s.t.\quad A_2^{\mathrm{ie}} y_{\mathrm{d}}^{(J)} + A_3^{\mathrm{ie}} y_{\mathrm{c}}^{(J)} - A_\sigma \sigma^{(J)} \le b^{\mathrm{ie}} - A_1^{\mathrm{ie}}\hat{x}^{(I)} \tag{33}$$
$$A_2^{\mathrm{eq}} y_{\mathrm{d}}^{(J)} + A_3^{\mathrm{eq}} y_{\mathrm{c}}^{(J)} = b^{\mathrm{eq}} - A_1^{\mathrm{eq}}\hat{x}^{(I)} + A_u\hat{u}^{(J)}$$

C. Solution Method

The MP and SP-L in (28) and (33), respectively, are MILP problems that can be solved efficiently with current commercial solvers. Due to the product terms of u and $\mu^{(j)}$ in (32), the SP-U in (31) is a bilinear programming problem (BLP). Although the BLP is nonlinear and nonconvex, various algorithms have been proposed to address it. The alternating direction (AD) algorithm, suggested in [28, 29], is employed in this paper. This is used to iteratively solve LP problems with $\mu^{(j)}$ and u fixed alternatively, as shown in (34) and (35), respectively. A decomposition strategy is used in (35), thus $\varsigma(\hat{x}^{(I)}, \hat{y}_{\mathrm{d}}^{(j)}, \hat{u})$ can be solved independently for each j. The objective value is then obtained by computing their maximum values.

$$\hat{\kappa}^{(I)} + \max_{\theta,u}\ \eta$$
$$s.t.\quad \eta \le \hat{\mu}^{(j)T}A_u u + \left(b^{\mathrm{ie}} - A_1^{\mathrm{ie}}\hat{x}^{(I)} - A_2^{\mathrm{ie}}\hat{y}_{\mathrm{d}}^{(j)}\right)^T \hat{\lambda}^{(j)} + \left(b^{\mathrm{eq}} - A_1^{\mathrm{eq}}\hat{x}^{(I)} - A_2^{\mathrm{eq}}\hat{y}_{\mathrm{d}}^{(j)}\right)^T \hat{\mu}^{(j)} \tag{34}$$
$$u \in U$$
$$\forall j = 1,2,...,J$$
$$\max\left\{\hat{\kappa}^{(I)} + \varsigma\left(\hat{x}^{(I)}, \hat{y}_{\mathrm{d}}^{(j)}, \hat{u}\right), \forall j = 1,2,...,J\right\} \tag{35}$$

D. Steps of the Algorithm

Finally, the improved nested C&CG algorithm is implemented as follows:

Step 1: Set the initial values of the outer loop $UB_{\mathrm{outer}} = +\infty$, $LB_{\mathrm{outer}} = -\infty$, and set the iteration counter of the outer loop $I = 1$.

Step 2: Solve MP denoted by (28), update LB_{outer}, get the planning decision variable values $\hat{x}^{(I)}$, and set the initial values of the inner loop $UB_{\mathrm{inner}} = +\infty$, $LB_{\mathrm{inner}} = -\infty$, and set the iteration counter of the inner loop $J = 1$.

Step 3: Solve SP-U iteratively using (34) and (35), update UB_{inner}, and get the discrete operational variable values $y_{\mathrm{d}}^{(J)}$.

Step 4: Solve SP-L using (33), update LB_{inner}, and get the uncertain variable values $\hat{u}^{(J)}$.

Step 5: If $UB_{\mathrm{inner}} - LB_{\mathrm{inner}} < \varepsilon_{\mathrm{inner}}$, update UB_{outer}, and go to Step 6; otherwise, update $J = J + 1$, and go to Step 3.

Step 6: If $UB_{\mathrm{outer}} - LB_{\mathrm{outer}} < \varepsilon_{\mathrm{outer}}$, print the investment decision $\hat{x}^{(i)}$ and terminate; otherwise, update $I = I + 1$, and go to Step 2.

IV. Case Study

The modified Garver's 6-bus system and a practical Chinese 196-bus system are used to verify the advantages of the proposed formulation and the efficiency of the improved nested C&CG algorithm. The effects of energy storage investment on relieving transmission line congestion and reducing investment cost of transmission lines are analyzed in this section.

The MILP and LP problems were solved using Cplex 12.8 [30] on a computer with dual Intel Xeon CPU E5-2650 and 128GB RAM.

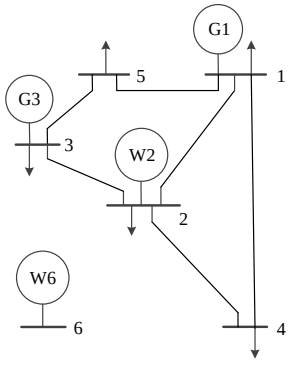

Fig. 1. Garver's 6-bus system.

A. Modified Garver's 6-Bus System

The modified Garver's 6-bus system, as shown in Fig. 1, contains 2 conventional generators with 600 MW total capacity, and 15 candidate transmission lines with 6 already built. In

order to verify the proposed method, 2 wind farms are added at buses 2 and 6, with capacities of 100 MW and 450 MW, respectively. The detailed data for this system is provided in the Appendix.

1) Effect of Energy Storage on Relieving Transmission Line Congestion

TABLE I
PLANNING RESULTS OF GARVER'S 6-BUS SYSTEM

Scheme	Annualized Invest. Cost ($10^6$$)			Planning Decision
	Lines	ESs	Total	
transmission expansion planning (without ES)	190	-	190	Line 2-3 ×1, Line 2-6 ×3, Line 3-5 ×1, Line 4-6 ×2
co-planning (with ES)	110	47.5	157.5	Line 2-6 ×3, Line 3-5 ×1 ES at Bus 6 (142.74MW, 874.61MW·h, Pb-C Bat.)

The co-planning results are shown in TABLE I. The transmission expansion planning scheme without candidate energy storage is also presented for comparison. One can see from the planning decision that 3 new transmission lines are not required if energy storage is built at bus 6, which verifies the role of energy storage in reducing additional transmission line construction.

In fact, the main transmission issue in this system is to transfer power generated by wind farm W6 to the loads distributed in the remainder of the system. Fig. 2 shows the total power flow of transmission lines connected to bus 6 in the worst-case scenarios. Co-planning eliminates the construction cost of 2 transmission lines connected to bus 6 with the price of installing an energy storage at bus 6. Wind power exported from bus 6 exceeds 300MW (equal to the capacity of 3 transmission lines) in a relatively short portion during the day. Therefore, energy storage can shift the peak loading power of transmission lines to light loading time periods.

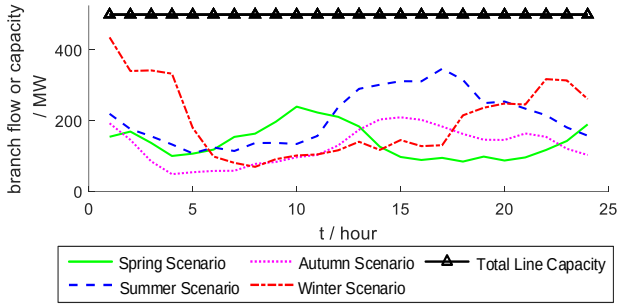

(a) Transmission expansion planning (without ES)

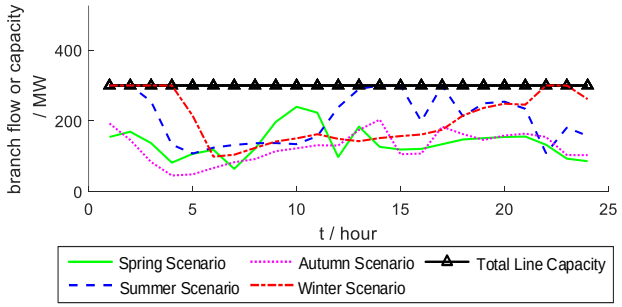

(b) Co-planning (with ES)

Fig. 2. Total power flow of transmission lines connected to bus 6.

Energy storage can be used to relieve transmission line congestion. However, in this test system, it is difficult to conduct serious economic plausibility analysis due to the use of potentially unrealistic cost data. Whether energy storage is economical for reducing transmission line investment cost will be analyzed in a practical Chinese system.

2) Advantages of the Proposed Formulation

The proposed formulation (denoted as 'proposed' in TABLE II) takes operational binary variables for energy storages as second stage variables, i.e., 'wait and see' variables. While some existing formulations adopted in [16] and [19] (denoted as 'existing' in TABLE II) modeled these binary variables as first stage variables, i.e., 'here and now' variables. In order to demonstrate the drawbacks of determining energy storage statuses in the planning phase, a special scenario is considered in the numerical simulation. The results indicate that existing formulations might underestimate the flexibility of energy storage in managing renewable generation uncertainty, which possibly leads to unnecessary investment, or even makes the problem infeasible in the case that a solution exists.

For a clearer description, only one scenario with a special feature (shown in Fig. 3) is considered in both formulations. The main feature of this scenario is that it requires an energy storage to charge in one realization of wind power uncertainty and to discharge in another one within the same time period. Three cases with different settings for candidate energy storages and transmission lines are tested, and the co-planning results are shown in TABLE II.

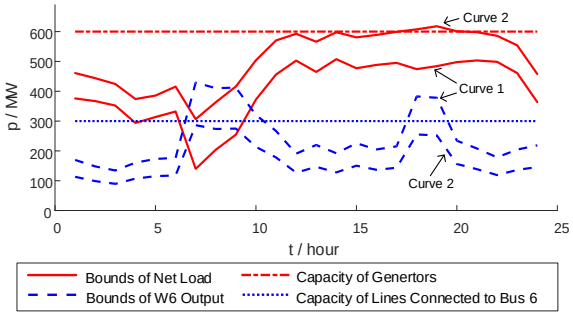

Fig. 3. Wind power at bus 6 and system net load power.

Case 1 takes the same settings for candidate transmission lines and energy storages as those shown in TABLE IX and TABLE X. The existing formulation results in an additional energy storage being built at bus 6. Realization of curve 1 in Fig. 3 requires energy storage charging due to line congestion at hours 18 and 19, while the realization of curve 2 requires energy storage discharging due to temporary overload (i.e., the system load exceeds the capacity of generators) during the same time period. As a result, determining energy storage statuses in the planning phase cannot simultaneously address both types of uncertainty realizations. In order to 'separate' charge and discharge actions, two energy storages are selected in the results from the existing formulation. However, only one is required to cope with both realizations and the proposed formulation offers reasonable results.

Case 2 includes only one candidate energy storage, i.e., a lead-carbon (Pb-C) battery at bus 6, while the remaining input data matches that in case 1. The results from the existing formulation in TABLE II indicate that one additional transmission line connected to bus 6 is required to handle the congestion, and energy storage at bus 6 is used to cope with the peak load. For the same reason as in case 1, redundant investment is made under the existing formulation when operational variables are determined in the planning stage.

Case 3 limits the maximum number of candidate transmission lines 2-6 and 4-6 to 3 based on the settings of case 2. The existing formulation is infeasible, although a solution exists for this case.

TABLE II
COMPARISON OF PLANNING RESULTS FOR DIFFERENT FORMULATIONS

Model	Case	Annualized Invest. Cost ($10^6$$)			Planning Decision
		Lines	ESs	Total	
proposed	all	130	27.9	157.9	Line 2-3 ×1, Line 3-5 ×1, Line 4-6 ×3, ES at Bus 6 (136.05MW, 378.69MW·h, Pb-C Bat.)
existing	case 1	130	33.6	163.6	Line 2-3 ×1, Line 3-5 ×1, Line 4-6 ×3, ES at Bus 6 (22.62 MW,29.84MW·h, $LiFePO_4$ Bat.), ES at Bus 6 (136.05MW, 378.69MW·h, Pb-C Bat.)
	case 2	160	16.6	176.6	Line 2-3 ×1, Line 3-5 ×1, Line 2-6 ×2, Line 4-6 ×2, ES at Bus 6 (136.05MW, 378.69MW·h, Pb-C Bat.)
	case 3	infeasible			-

Therefore, compared with existing formulations that decide energy storage statuses in the planning phase, the proposed formulation can properly reflect the flexibility of energy storage in the operational phase, in order to address renewable generation uncertainty.

B. Practical Chinese 196-Bus System

The practical Chinese 196-bus system consists of two provincial power grids as shown in Fig. 4. One province is located in northwest China with large capacities of wind and solar generation. The other province is located in central China with a larger population and heavier electricity demands. Two regions are connected with a 2383 km high voltage direct current (HVDC) transmission line to transfer clean energy from the northwest China province (NWCP) to the central China province (CCP).

1) System Description

The system includes 196 buses (including 23 buses of 750 kV, 114 buses of 330 kV, 42 buses of 500 kV and 17 transformer neutral buses), 371 AC transmission lines, 1 cross-regional HVDC transmission line, and 192 conventional generators with 44776.60 MW of installed capacity. The power grid of CCP contains an existing 1200 MW pumped storage. The power grid of NWCP contains 20368.70MW of renewable power generation capacity.

Robust co-planning of energy storage and transmission line was conducted based on the long-term prediction. For the sake of avoiding synchronous interconnections between different regional grids, candidate tie lines are set as HVDC transmission lines. Candidate types of energy storage are lead-carbon (Pb-C) battery, lithium iron phosphate ($LiFePO_4$) battery and pumped storage. Candidate locations are determined by the system integration criteria, available natural resources, and experience of engineers. Parameters for candidate tie lines and energy storages are summarized in TABLE III and TABLE IV.

TABLE III
PARAMETERS FOR CANDIDATE TIE LINES IN 196-BUS SYSTEM

No.	From Bus	To Bus	Capacity (MW)	Voltage Level (kV)	Annualized Cons. Cost (10^8CNY)
HVDC 1	125	192	8000	±800	5.24
HVDC 2	125	192	6000	±800	4.58
HVDC 3	125	192	4000	±600	3.60
HVDC 4	125	192	3000	±600	3.30

TABLE IV
PARAMETERS FOR CANDIDATE ENERGY STORAGE IN 196-BUS SYSTEM

Type	η_i^{ch} / η_i^{dc}	Annualized Cons. Cost			Candidate Bus
		α_i	β_i	χ_i	
Pb-C Bat.	0.92	250	250	0.16	1, 5, 17, 31, 46, 125
$LiFePO_4$ Bat.	0.95	167	417	0.16	1, 5, 17, 31, 46, 125
Pumped Stor.	0.90	120	2	0.2	196

Units of α_i, β_i, and χ_i, and are CNY/kW, CNY/kW·h and 10^8 CNY, respectively.

2) Planning Results

TABLE V shows planning results for the practical Chinese 196-bus system. Congestion in this system arises when the output from wind farms in NWCP is large in some periods and the existing cross-regional HVDC lacks available capacity to relieve this congestion. Therefore, energy storage absorbs the redundant wind generation in these periods and releases this power when HVDC is lightly loaded. Compared with constructing another HVDC line, energy storage investment enjoys the advantage of saving total cost in this case with over 2000 km transmission distance. The pumped storage at bus 196 eliminates the requirement for a new cross-regional HVDC transmission line.

TABLE V
PLANNING RESULTS FOR 196-BUS SYSTEM

Model	Annualized Invest. Cost (10^8CNY)			Planning Decision
	Lines	ESs	Total	
transmission expansion planning (without ES)	3.46	-	3.46	Line 17-125 ×1, Line 161-164 ×1, Line 164-192 ×1, HVDC 4 ×1
co-planning (with ES)	0.20	2.05	2.25	Line 67-66 ×1, Line 31-196, ES at Bus 196 (1486.5MW, 3230.7MW·h, Pumped Storage)

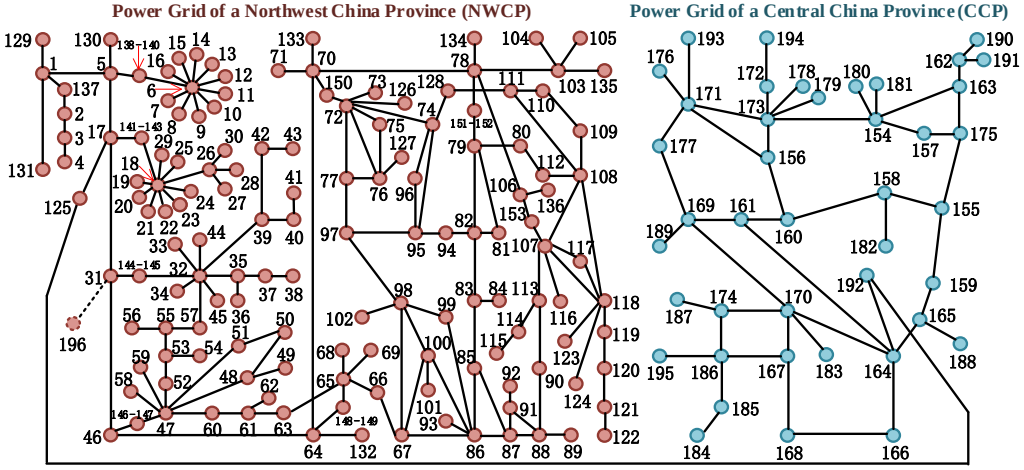

Fig. 4 Topology of practical Chinese 196-bus system.

3) Sensitivity Analysis

Sensitivity analysis was conducted in order to test the robustness of the planning results. Critical coefficients selected for analysis include line cost per unit length C_{line} and converter cost C_{conv} for HVDC, as well as cost per unit power capacity α and per unit energy capacity β for energy storage. Comparisons of annualized investment cost of HVDC and pumped storage are summarized in Fig. 5, given different values of the above coefficients. The overall investment is affected by the per power capacity cost of pumped storage α at its change rate. The choice between HVDC and pumped storage in current planning results would switch if α incensed by 70% or C_{line} decreased by 50%.

Given the expectation of cost decrease in the future battery storage industry, battery cost coefficients are analyzed as shown in Fig. 6. In contrast to pumped storage, the cost per unit energy capacity β is a more sensitive coefficient in the investment of battery storage. As indicated, batteries would be chosen to relieve transmission congestion in this system, when β for Pb-C batteries and $LiFePO_4$ batteries reaches approximately 30% and 20% of their current values, respectively.

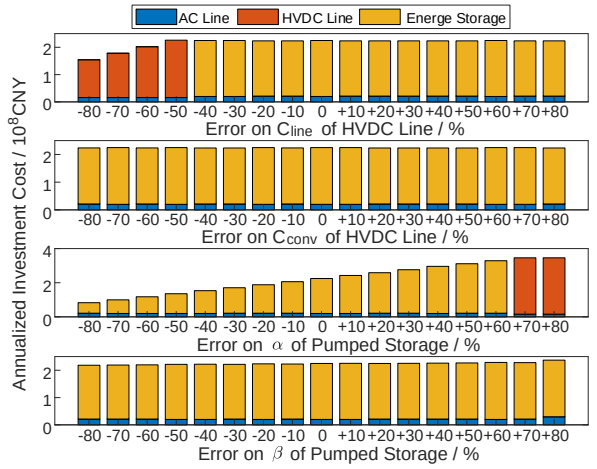

Fig. 5 Analysis on cost coefficients for HVDC line and pumped storage.

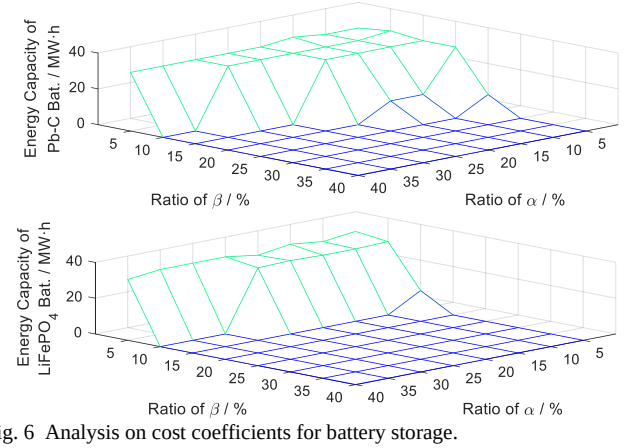

Fig. 6 Analysis on cost coefficients for battery storage.

4) Effect of Energy Storage on Reducing Transmission Line Investment Cost

One may consider under what circumstances energy storage investment is economical for relieving congestion compared with installing transmission lines. In this practical system with 2383 km transmission distance between two provincial power grids, transmission line cost increases with its length, and exceeds energy storage investment cost after a certain transmission distance. Using the method proposed in this work, investment costs of energy storages and transmission lines were compared for different transmission distances. The annualized construction cost of an HVDC system is defined in (36).

$$C_i^{\text{cons}} = C_{\text{line}\,i} \cdot l_i + 2 \cdot C_{\text{conv}\,i} \quad i \in \Omega_{\text{ndl}} \tag{36}$$

Results in Fig. 7 indicates that the energy storage investment cost almost remains constant for different transmission distances, while transmission line cost increases with transmission distance. In this system, if the transmission distance between two regions was less than 1250 km, the co-planning problem would choose to install an HVDC; otherwise, energy storage is chosen for investment. Thus, the transmission distance is a critical factor determining the economic plausibility of energy storage investment for reducing transmission line construction cost. Energy storage investment is economical under the condition that the transmission distance is long enough to make the construction cost of lines exceed that of energy storages.

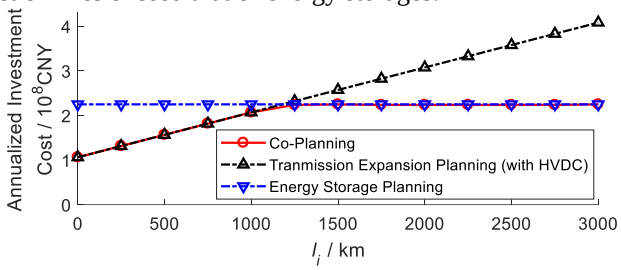

Fig. 7. Cost of energy storage and transmission line.

C. Algorithm Performance Improvement

TABLE VI and TABLE VII summarize computation time for the improved nested C&CG algorithm (denoted as 'improved') and the basic version in [23] (denoted as 'basic ver.'). SP-U of the basic version algorithm requires much more time compared with the other sub-problems. The original algorithm cannot address this problem with a few scenarios and a few time periods within an hour. However, the improved algorithm significantly reduces the computation time of the slave problem, thus reducing the total time.

TABLE VI
COMPARISON OF COMPUTATION TIME FOR MODIFIED GARVER'S SYSTEM

N_s	N_t	Alg.	Obj. (10^6\$)	Computation Time (sec)			
				MP	SP-U	SP-L	Total
1	1	basic ver.	172.1	0.5	1.1	0.4	2.0
		improved	172.1	1.5	0.7	0.8	3.0
1	2	basic ver.	174.2	0.9	14.5	0.4	15.8
		improved	174.2	1.3	0.8	0.8	2.9
1	6	basic ver.	-	>1.4	>3600	>1.0	>3600
		improved	166.6	1.4	0.5	0.5	2.4
4	24	basic ver.	-	>12.9	>3600	>0.6	>3600
		improved	330.5	140.4	2.3	2.4	145.0

TABLE VII
COMPARISON OF COMPUTATION TIME FOR 196-BUS SYSTEM

N_s	N_t	Alg.	Obj. (10^8¥)	Computation Time (sec)			
				MP	SP-U	SP-L	Total
1	1	basic ver.	-	>0.3	>3600	>0.1	>3600
		improved	0.435	2.1	0.7	0.7	3.6
4	24	basic ver.	-	>26.1	>3600	>4.2	>3600
		improved	6.648	200.6	19.9	12.5	232.9

V. CONCLUSION

This paper presented a robust formulation for energy storage and transmission line co-planning with mixed integer recourse. An improved nested C&CG algorithm was employed to solve the problem. The main conclusions of this work include:

1) The proposed formulation can properly reflect the flexibility of energy storage in the operational phase, in order to address renewable generation uncertainty. This offers more reasonable planning results compared with previous formulations, where energy storage statuses are determined in the planning phase.
2) The improved nested C&CG algorithm relieves numerical issues caused by a large number of new binary variables, big-M constraints, and large problem size in the SP of the basic version algorithm. A significant reduction in computation time was verified in the results from the case study.
3) The numerical results for the practical 196-bus system indicate that investment in energy storage is more economical for alleviating transmission congestion, compared to building a new long-distance transmission line.

APPENDIX

Parameters for modified Garver's 6-bus system are listed in TABLE VIII, TABLE IX, and TABLE X.

TABLE VIII
PARAMETERS FOR GENERATORS IN MODIFIED GARVER'S SYSTEM

Generator	Bus	$\overline{P}_i$ (MW)	$\underline{P}_i$ (MW)	RU_i (MW/h)	RD_i (MW/h)
G1	1	200.0	0.0	100	100
G3	3	400.0	0.0	200	200

TABLE IX
PARAMETERS FOR CANDIDATE LINES IN MODIFIED GARVER'S SYSTEM

From Bus	To Bus	Reactance (p.u.)	Capacity (MW)	Annualized Cons. Cost (10^6\$)	# of Lines Already Built
1	2	0.4	100	40	1
1	3	0.38	100	38	0
1	4	0.6	80	60	1
1	5	0.2	100	20	1
1	6	0.68	70	68	0
2	3	0.2	100	20	1
2	4	0.4	100	40	1
2	5	0.31	100	31	0
2	6	0.3	100	30	0
3	4	0.59	82	59	0
3	5	0.2	100	20	1
3	6	0.48	100	48	0
4	5	0.63	75	63	0
4	6	0.3	100	30	0
5	6	0.61	78	61	0

TABLE X
PARAMETERS FOR CANDIDATE STORAGES IN MODIFIED GARVER'S SYSTEM

Type	η_i^{ch} / η_i^{dc}	Annualized Cons. Cost		
		α_i (\$/kW)	β_i (\$/kW·h)	χ_i (10^6\$)
Pb-C Bat.	0.92	39	39	7.8
$LiFePO_4$ Bat.	0.95	26	65	5.2

ACKNOWLEDGMENT

The authors would like to thank Dr. Lei Fan for the helpful discussion.

REFERENCES

[1] L. L. Garver, "Transmission Network Estimation Using Linear Programming," *IEEE Transactions on Power Apparatus and Systems*, vol. PAS-89, pp. 1688-1697, 1970.
[2] R. Villasana, L. L. Garver and S. J. Salon, "Transmission Network Planning Using Linear Programming," *IEEE Transactions on Power Apparatus and Systems*, vol. 104, pp. 349-356, 1985.
[3] R. Romero, R. Gallego and A. Monticelli, "Transmission system expansion planning by simulated annealing," *IEEE Transactions on Power Systems*, vol. 11, pp. 364-369, 1996.
[4] L. Bahiense, G. C. Oliveira, M. Pereira, and S. Granville, "A Mixed Integer Disjunctive Model for Transmission Network Expansion," *IEEE Power Engineering Review*, vol. 21, p. 60-60, 2001.
[5] G. Latorre, R. D. Cruz, J. M. Areiza, and A. Villegas, "Classification of publications and models on transmission expansion planning," *IEEE Transactions on Power Systems*, vol. 18, pp. 938-946, 2003.
[6] Y. Li and J. D. McCalley, "Design of a High Capacity Inter-Regional Transmission Overlay for the U.S.," *IEEE Transactions on Power Systems*, vol. 30, pp. 513-521, 2015.
[7] S. Chakraborty, T. Senjyu, H. Toyama, A. Y. Saber, and T. Funabashi, "Determination methodology for optimising the energy storage size for power system," *IET Generation, Transmission & Distribution*, vol. 3, pp. 987-999, 2009.
[8] M. Ghofrani, A. Arabali, M. Etezadi-Amoli, and M. S. Fadali, "A Framework for Optimal Placement of Energy Storage Units Within a Power System With High Wind Penetration," *IEEE Transactions on Sustainable Energy*, vol. 4, pp. 434-442, 2013.
[9] S. Wogrin and D. F. Gayme, "Optimizing Storage Siting, Sizing, and Technology Portfolios in Transmission-Constrained Networks," *IEEE Transactions on Power Systems*, vol. 30, pp. 3304-3313, 2015.
[10] Z. Hu, F. Zhang and B. Li, "Transmission expansion planning considering the deployment of energy storage systems," in *2012 IEEE Power and Energy Society General Meeting*, 2012, pp. 1-6.
[11] F. Zhang, Z. Hu and Y. Song, "Mixed-integer linear model for transmission expansion planning with line losses and energy storage systems," *IET Generation, Transmission & Distribution*, vol. 7, pp. 919-928, 2013.
[12] M. Hedayati, J. Zhang and K. W. Hedman, "Joint transmission expansion planning and energy storage placement in smart grid towards efficient integration of renewable energy," in *2014 IEEE PES T&D Conference and Exposition*, 2014, pp. 1-5.
[13] J. A. Aguado, S. de la Torre and A. Triviño, "Battery energy storage systems in transmission network expansion planning," *Electric Power Systems Research*, vol. 145, pp. 63-72, 2017.
[14] A. J. Conejo, Y. Cheng, N. Zhang, and C. Kang, "Long-term coordination of transmission and storage to integrate wind power," *CSEE Journal of Power and Energy Systems*, vol. 3, pp. 36-43, 2017.
[15] T. Qiu, B. Xu, Y. Wang, Y. Dvorkin, and D. S. Kirschen, "Stochastic Multi-Stage Co-Planning of Transmission Expansion and Energy Storage," *IEEE Transactions on Power Systems*, vol. 32, pp. 643-651, 2017.
[16] S. Dehghan and N. Amjady, "Robust Transmission and Energy Storage Expansion Planning in Wind Farm-Integrated Power Systems Considering Transmission Switching," *IEEE Transactions on Sustainable Energy*, vol. 7, pp. 765-774, 2016.
[17] F. Maggioni, F. A. Potra and M. Bertocchi, "Stochastic versus Robust Optimization for a Transportation Problem,", [Online]. Available: http://www.optimization-online.org/DB_FILE/2015/03/4805.pdf 2014.
[18] B. Zhou, G. Geng and Q. Jiang, "Hierarchical Unit Commitment With Uncertain Wind Power Generation," *IEEE Transactions on Power Systems*, vol. 31, pp. 94-104, 2016.
[19] R. A. Jabr, I. Dzafic and B. C. Pal, "Robust Optimization of Storage Investment on Transmission Networks," *IEEE Transactions on Power Systems*, vol. 30, pp. 531-539, 2015.
[20] R. A. Jabr, "Robust Transmission Network Expansion Planning With Uncertain Renewable Generation and Loads," *IEEE Transactions on Power Systems*, vol. 28, pp. 4558-4567, 2013.
[21] S. Dehghan, N. Amjady and A. Kazemi, "Two-Stage Robust Generation Expansion Planning: A Mixed Integer Linear Programming Model," *IEEE Transactions on Power Systems*, vol. 29, pp. 584-597, 2014.
[22] D. Bertsimas, E. Litvinov, X. A. Sun, J. Zhao, and T. Zheng, "Adaptive Robust Optimization for the Security Constrained Unit Commitment Problem," *IEEE Transactions on Power Systems*, vol. 28, pp. 52-63, 2013.
[23] L. Zhao and B. Zeng, "An Exact Algorithm for Two-stage Robust Optimization with Mixed Integer Recourse Problems,", University of South Florida Technical Report, 2012.
[24] B. Zeng, "Solving Two-stage Robust Optimization Problems by A Constraint-and-Column Generation Method," *Operations Research Letters*, vol. 41, pp. 457-461, 2013.
[25] Renewable Energy Law of the People's Republic of China, [Online]. Available: http://english.gov.cn/archive/laws_regulations/2014/08/23/content_281474983043598.htm
[26] State Council of the People's Republic of China Order No. 599, Regulations on Emergency Handling, Investigation and Disposal of Electric Power Safety Accidents, [Online]. Available: http://www.gov.cn/flfg/2011-07/15/content_1908466.htm

[27] L. Han and Z. Dong, "Legislative background, characteristics and improvement of Chinese Regulations on Emergency Handling, Investigation and Disposal of Electric Power Safety Accidents," in *2012 China International Conference on Electricity Distribution*, 2012, pp. 1-4.
[28] R. Jiang, M. Zhang, G. Li, and Y. Guan, "Two-Stage Robust Power Grid Optimization Problem,", University of Florida Technical Report, 2014.
[29] A. Lorca and X. A. Sun, "Adaptive Robust Optimization With Dynamic Uncertainty Sets for Multi-Period Economic Dispatch Under Significant Wind," *IEEE Transactions on Power Systems*, vol. 30, pp. 1702-1713, 2015.
[30] ILOG CPLEX Homepage, [Online]. Available: http://www.ilog.com

Siyuan Wang received his B.S. degree from Zhejiang University, Hangzhou, China, in 2013, where he is currently pursuing the Ph.D. degree in electrical engineering.

His research interests include power system optimization, renewable energy integration and the application of energy storage technology in power systems.

Guangchao Geng (S'10-M'14) received his B.S. and Ph.D. degrees in electrical engineering from the College of Electrical Engineering, Zhejiang University, Hangzhou, China, in 2009 and 2014, respectively. From 2012 to 2013, he was a visiting student at the Department of Electrical and Computer Engineering, Iowa State University, Ames, United States. From 2014 to 2017, he is a post-doctoral fellow at the College of Control Science and Engineering, Zhejiang University, Hangzhou, China and the Department of Electrical and Computer Engineering, University of Alberta, Edmonton, AB, Canada.

Currently, he is an assistant research fellow at the College of Electrical Engineering, Zhejiang University, Hangzhou, China. His research interest includes power system stability and control, renewable energy integration, and high performance computing.

Quanyuan Jiang (M'10) received his B.S., M.S., and Ph.D. degrees in electrical engineering from Huazhong University of Science & Technology, Wuhan, China in 1997, 2000, and 2003, respectively. From 2006 to 2008, he was a visiting associate professor at the School of Electrical and Computer Engineering, Cornell University, Ithaca, United States.

He is currently a professor at the College of Electrical Engineering, Zhejiang University, Hangzhou, China. His research interest includes power system stability and control, high performance computing, and applications of energy storage systems in power systems.